

## Active Magnetic Bearing Design Optimization and Transient-State Analysis Using ANSYS

Dr. Adil H. Ahmed \* & Dr. Thamir M. Abdul Wahab<sup>1</sup>

Received on: 23/6 /2009

Accepted on: 3/ 6/2010

### Abstract

This paper presents design optimization, and transient-state analysis of active magnetic bearings (AMB) using the powerful ANSYS software package. ANSYS software provides the required environment for numerical modeling and analysis based on the finite element method (FEM). In this paper two programs are developed in ANSYS, the first for modeling and optimizing the analytically designed active magnetic bearing, and the second for transient-state analysis of the FE model to investigate the effects of eddy currents on the considered active magnetic bearing.

**Keywords:** Active magnetic bearing (AMB), Finite element method (FEM), ANSYS software package.

### التصميم الأمثل و تحليل الحالة العابرة للمساند المغناطيسية الفعالة باستخدام برمجيات ANSYS

#### خلاصه

يقدم هذا البحث التصميم الأمثل و تحليل الحالة العابرة للمساند المغناطيسية الفعالة (AMB) باستخدام حقيبة البرمجيات ANSYS ذات القدرات العالية, حيث توفر برمجيات ANSYS البيئة المطلوبة للنمذجة و التحليل الرقمي باستعمال طريقه العناصر المحددة (FEM).

في هذا البحث تم بناء برنامجين باستخدام لغة ANSYS, البرنامج الأول هو لعمل نموذج حاسوبي للمسنند المغناطيسي الفعال الذي سبق تصميمه بالطرق التحليلية ثم إجراء الحسابات اللازمة عليه للوصول إلى التصميم الأمثل, و البرنامج الثاني هو لتحليل الحالة العابرة باستخدام النموذج الحاسوبي لبحث تأثيرات التيارات الدوامة على المسند المغناطيسي.

### 1. Introduction

An AMB is an electromagnetic device that uses actively controlled magnetic field for rotor suspension. AMBs are non-contact bearings, which enables very high-speed operation.

For the analysis of AMBs the numerical methods are more powerful and accurate than analytical methods. In this paper the

numerical FEM using the powerful ANSYS software package is the one depicted.

Design optimization is an advanced technique in ANSYS that can be used to optimize the AMB geometry. The objective of the analysis is to minimize the volume of the actuator with maintaining the maximum magnetic force higher than a specified limit. The optimization-program is

implemented on the selected AMB for two sets of design variables. The optimization results are given in table form and by colored graphs to show the changes made on the AMB geometry.

During rotation and following the vibrations in rotor, time varying control currents are superimposed on the actuator biasing current due to the control action. To investigate this situation the transient state analysis method in ANSYS is implemented on the FE model. The supply voltage is assumed to vary in steps with time so the analysis will track the coil currents, journal force and coil inductance over time in response to this applied voltage. These quantities will change slightly due to the development of eddy currents in the journal as shown clearly by the colored graphs of this analysis. The magnetic force, power loss, and energy stored in the journal due to the presence of this eddy current are computed.

## 2. Geometry optimization

Design optimization is a technique that seeks to determine an optimum design, that reaches the maximum bearing force but with a minimum possible volume of the entire construction. The ANSYS program performs a series of analysis-evaluation-modification cycles. This process is repeated until all specified criteria are met. The main steps in the design optimization program are explained by the flowchart in figure 3.

Using the ANSYS Parametric Design Language (APDL) all the numerical values must be entered to the program as variable parameters, table 1 or table 2. The program reads these scalar values assigned to the parametric variables and consider it as initial assumptions.

As design variables (DV) the following parameters are chosen, see figure (1) [2] [3]:

- 1- The pole width  $w$ .
- 2- The journal thickness  $w_j$ .
- 3- The stator yoke thickness  $w_s$ .
- 4- The axial length of the stator iron  $\ell_{ax}$ .
- 5- The nominal gap length  $g_o$ .

As state variables (SV), only  $F_{max}$  is chosen. Where the program calculates  $F_{max}$ , at the condition of  $i_1=i_2=I_b$ ,  $i_3=I_{max}$ , and  $i_4=0$ , See figure (b) [2] [3].

The chosen objective function is the total iron volume (IVOLU), including the journal plus the stator iron core.

For the magnetic force to be related only to iron volume the coils current density  $J_{max}$  is assumed to be constant that is when both maximum current density  $I_{max}$  and coil space area  $A_c$  are maintained constants.

The two selected AMBs listed in tables 1 and 2 are used as a two cases of design optimization. For each AMB two design-variables sets are chosen. In the first set the pole legs, the journal, and the stator yoke are assumed of equal width ( $w=w_j=w_s$ ), this assumption is to insure a uniform flux path along the magnetic circuit. In the second set each of these parameters is considered as an individual design-variable.

The optimization results are tabulated in tables 3 and 4 for AMB(1) and AMB(2), respectively. For set (1) it can be seen that the minimum volume obtained is larger than that of set (2) for both cases, because the program is limited by equal values of ( $w=w_j=w_s$ ), while in set (2) the program can freely reach different values for ( $w$ ,  $w_j$ , and  $w_s$ ), and therefore a lower minimum volume can be obtained. Consider table 3, AMB (1), for set (1) it can

be seen that the optimum result  $w=1.37$  is less than the designed value  $w=1.51$ , also  $\ell_{ax}=12$  cm is less than the designed value  $\ell_{ax}=13$  cm and the optimum volume  $I_{volu}=1640$  cm<sup>3</sup> is less than the designed value  $I_{volu}=1977$  cm<sup>3</sup>. However  $F_{max}$  is increased and this is because the gap length  $g_o$  is reduced from 0.6mm to 0.55 mm, since  $g_o$  is inversely proportional to  $F_{max}$ . The minimum acceptable  $g_o$  which is specified as a lower limit should be practically feasible. For set (2) the results show that  $w > w_s > w_j$ , also the axial length is reduced to 12 cm instead of 13 cm, and the volume is reduced to 1570 cm<sup>3</sup> with  $F_{max}$  higher than the lower limit. The air gap length is also computed as  $g_o=0.55$  mm that is less than the nominal value.

By referring to table 4, AMB (2), for set (1) the results show that the optimum value for  $w=0.65$  is less than the design value  $w=0.68$ , but the axial length  $\ell_{ax}=5$  cm is taller than the designed length  $\ell_{ax}=4.85$  cm. However the total volume is reduced from 154 cm<sup>3</sup> to 151 cm<sup>3</sup>. For set (2) the optimum values are  $w=0.85$ ,  $w_j=0.73$ , and  $w_s=0.78$ , it can be seen that the program usually attains values for  $w$  higher than that for  $w_j$  and  $w_s$  because it has direct impact on the generated magnetic force  $F_{max}$ . In this case the volume is less than that for set (1), the axial length is shorter, and  $g_o$  is the same for both sets.

For AMB (1); figure 6 (a) presents the designed geometry before optimization, the figure shows flux density  $B$  distribution inside the actuator when the maximum force  $F_{max}$  is generated at electromagnet 3. Figure 6 (b) presents the optimum results for set (1), a uniform distribution of  $B$  throughout the magnetic circuit can be seen in spite

of the reduction made in  $w$ ,  $w_j$ , and  $w_s$ . Figure 6(c) presents the optimum results for set (2),  $B$  is higher at the journal because  $w_j$  is less than  $w_s$  and  $w$ , which is undesirable. Since this means that the journal may reach saturation before the other parts of the actuator.

Figure 7 presents AMB (2) where (a) is the model of the designed geometry, and (b) and (c) are models of the optimized geometry for set (1) and (2) respectively. In figure 7 (b), since the magnetic circuit is uniform ( $w=w_j=w_s$ ), therefore  $B$  is uniformly distributed along the magnetic circuit although  $w$ ,  $w_j$ ,  $w_s$ ,  $\ell_{ax}$ , and the iron volume are reduced. In figure 7 (c),  $B$  is uniformly distributed with no saturation in the magnetic path although  $w_j$  is less than  $w_s$  and  $w$ . This indicates an acceptable optimum set.

By referring to tables 3 and 4, the following reduction in the overall iron volume is obtained: for AMB (1), the optimized volume is only 83% of the iron volume before optimization, this is for set (1), while for set (2) the ratio reduces to 80%. For AMB (2), the ratio is 98% and 97.3% respectively. There is a considerable difference between the two cases and this can be explained by referring to tables 3 and 4, we can see that AMB (1) is approximately twice in dimensions with respect to AMB (2), and the design results show that it is preferable to use 16-poles for this AMB instead of the chosen 8-poles configuration. So the design algorithm is accurate and gives good results when the free parameters are chosen properly as can be seen for AMB (2) where the design results are very close to the optimum one. So the optimization-program can verify and correct the designed AMB geometry.

### 3. Transient-state analysis

Magnetic fields caused by arbitrary electric current that varies over time can be analyzed using 2-D transient magnetic analysis. Using this type of analysis, time dependent effects such as eddy currents, power loss due to eddy currents, and magnetic forces induced by eddy currents can be treated. The same procedure used for the static magnetic analysis; of building the model geometry, assigning physics attributes, and meshing the model holds for this type of analysis. However a transient analysis involves boundary conditions and loads that are functions of time. To specify such loads the coils are supplied with an excitation voltage, which varies with time. This voltage increases from 0 volts to biasing supply voltage in three load steps over a 0.06 sec time (in the first load step the voltage ramps in five steps of 0.002 sec time, followed by two constant voltage steps over the time stepping ending at 0.03 and 0.06 seconds respectively).

The coil requires additional characterization, including cross-section area and fill factor. Resistivity for copper is also provided

( $\rho_{cu} = 3 \times 10^{-8} \Omega \cdot m$ ). The journal assumed to be solid steel, so it requires the input of electrical resistivity ( $\rho_{steel} = 70 \times 10^{-8} \Omega \cdot m$ ).

For AMB transient analysis, a program is developed in ANSYS, as illustrated by the flowchart given in figure 8.

This analysis is performed on AMB(1) with maximum supply voltage equals to 80 volts and biasing voltage equals to ( $\beta \times V_{max}$ ), where  $\beta = 0.315$ , and on AMB(2) with maximum supply voltage equals to 270 volts and biasing voltage equals

to ( $\beta \times V_{max}$ ), where  $\beta = 0.5$ . The two solutions use constant time stepping over three load steps ending at 0.01, 0.03, and 0.06 seconds respectively.

The results of the magnetic force, power loss, and energy stored in the journal of AMB (1) and AMB (2) are given in tables 5 and 6 respectively.

The power loss and energy stored in the journal are given per meter of axial length, where  $l_{ax} = 13.0211$  cm, therefore, the total power loss is:

$$P = 1329 \times 13.0211 \times 10^{-2} = 173 \text{ W}$$

And the energy loss, from the table, after 0.06 sec is:

$$J/m \times l_{ax} = 41.22 \times 13.0211 \times 10^{-2} = 5.37 \text{ J}$$

For AMB (2) the power loss and the energy stored are considerably less since the biasing power for AMB (1) is:

$$V \times I_b = 80 \times 31.46 = 2.517 \text{ kVA}$$

And for AMB (2) is:

$$V \times I_b = 270 \times 5 = 1.35 \text{ kVA}$$

Figure 9(a) present the transient effect of pushing the magnetic field represented by the 2D flux lines to the outer surface of the journal. Figure 9(b) and (c) shows the effect of the transient condition of concentrating the flux density at the outer surface of the journal, which leads to saturation at certain parts in the journal. In figure 10(d) the current density in each coil of AMB (1) is shown. The current in direction  $+J_z$  is indicated by red color and the current in direction  $-J_z$  is indicated by blue color. The interesting thing in this figure, which differs from the results obtained from steady-state analysis, are the green dots, which indicate the presence of current density in the journal. This current density indicates clearly the generation of eddy current in the journal due to the transient effects. Figure 11 shows the same effects

noticed in AMB (2) but with less power.

#### 4. Conclusions

- The AMB geometry optimization objective is to find the minimum volume of the overall iron (the journal plus the stator) at a certain magnetic force (not less than  $F_{max}$ ).

The results of the *optimization* program show that an 80-83% reduction in iron volume for AMB (1) is obtained, while for AMB (2) the obtained reduction in iron volume is 97.3-98%. A small difference between the designed and the optimized volume indicates a good choice of free parameters during the design process.

- The *FEM transient-state* analysis program simulates the transient conditions to investigate the development of eddy currents in the journal. Accordingly the power loss and energy stored in the journal due to this current is computed.

Also the distortion in flux density in the journal due to the development of eddy current and the place of formation and density of this current are well shown in the resultant figures with their associated numerical values.

#### References

- [1] ANSYS Help Documentation, version (9).
- [2] Adil H. Ahmed and Thamir M. Abdul-wahab, "Analysis and Design of an Active Magnetic Bearing", Ph.D. Thesis, University of Technology, Baghdad, Iraq, 2009.
- [3] Adil H. Ahmed and Thamir M. Abdul-wahab, "Analysis and Design

of Radial Active Magnetic Bearings", The 6<sup>th</sup> Engineering Conference College of Engineering/ University of Baghdad, 5-7 April 2009, vol. 4, p.97-124.

[4] Boštjan Polajžer, "Design and Analysis of an Active Magnetic Bearing Experimental System", Ph.D. Dissertation, University of Maribor, Slovenia, 2003.

[5] Eric Maslen, "Magnetic Bearings", University of Virginia, 2000.

[6] Matti Antila, Erkki Lantto, and Antero Arkkio, "Determination of Forces and Linearized Parameters of Radial Active Magnetic Bearings by Finite Element Technique," IEEE Transactions on Magnetics, Vol. 34, No. 3, May 1998.

[7] Adam Pilat, "FEMLAB Software Applied to Active Magnetic Bearing Analysis", Int. J. Appl. Math. Comput. Sci., 2004, Vol. 14, No. 4, 497-501.

[8] Jeffrey D. Lindlau and Carl R. Knospe, "Feedback Linearization of an Active Magnetic Bearing with Voltage Control", IEEE Transactions on Control Systems Technology, Vol. 10, No. 1, Jan. 2002.

**Table (1) Analytically designed parameters of AMB(1) [3], used as initial guess for the optimization program.**

| Results                          | Parameter (unit)         | 8-pole  |
|----------------------------------|--------------------------|---------|
| Air gap area                     | $A_g$ (cm <sup>2</sup> ) | 19.6694 |
| Pole width                       | $w$ (cm)                 | 1.51057 |
| Axial pole length                | $\ell_{ax}$ (cm)         | 13.0211 |
| Journal radius                   | $r_j$ (cm)               | 6.51057 |
| Stator (pole face) inner radius  | $r_p$ (cm)               | 6.57057 |
| Biasing ratio                    | $\beta$                  | 0.31464 |
| Coil thickness                   | $t_c$ (cm)               | 1.96633 |
| Coil height                      | $\ell_c$ (cm)            | 0.79235 |
| Coil area                        | $A_c$ (cm <sup>2</sup> ) | 1.55803 |
| Stator yoke inner-radius         | $r_c$ (cm)               | 7.84983 |
| Pole length                      | $\ell_p$ (cm)            | 1.27926 |
| Stator outer radius              | $r_s$ (cm)               | 9.3604  |
| Stator outer diameter            | $d_s$ (cm)               | 18.7208 |
| Stator axial length              | $\ell_s$ (cm)            | 16.9538 |
| Calculated amplifier capacity    | $VA_{max}$ (VA)          | 6674.24 |
| Capacity of the picked amplifier | KVA                      | 8       |
| Peak amplifier current           | $I_{max}$ (A)            | 100     |
| Number of windings per pole      | $N$                      | 10.5042 |
| Biasing current                  | $I_b$ (A)                | 31.4643 |
| Area of copper wire              | $A_{cu}$ (mm)            | 7.4162  |
| Inductance per electromagnet     | $L$ (mH)                 | 0.997   |
| RMS current                      | $I_{rms}$ (A)            | 44.4972 |

**Table (2) Analytically designed parameters of AMB(2) [3], used as initial guess for the optimization program.**

| Results                         | Parameter (unit)         | 8-pole   |
|---------------------------------|--------------------------|----------|
| Air gap area                    | $A_g$ (cm <sup>2</sup> ) | 3.2994   |
| Pole width                      | $w$ (cm)                 | 0.679132 |
| Axial pole length               | $\ell_{ax}$ (cm)         | 4.85826  |
| Journal radius                  | $r_j$ (cm)               | 2.42913  |
| Stator (pole face) inner radius | $r_p$ (cm)               | 2.46913  |
| Biasing ratio                   | $\beta$                  | 0.335683 |
| Coil thickness                  | $t_c$ (cm)               | 0.683182 |
| Coil height                     | $\ell_c$ (cm)            | 0.958473 |
| Coil area                       | $A_c$ (cm <sup>2</sup> ) | 0.654811 |
| Stator yoke inner-radius        | $r_c$ (cm)               | 3.57694  |
| Pole length                     | $\ell_p$ (cm)            | 1.10781  |
| Stator outer radius             | $r_s$ (cm)               | 4.25607  |
| Stator outer diameter           | $d_s$ (cm)               | 8.51214  |
| Stator axial length             | $\ell_s$ (cm)            | 6.22463  |
| Calculated amplifier capacity   | $VA_{max}$ (VA)          | 2979     |

|                              |                             |          |
|------------------------------|-----------------------------|----------|
| Capacity of the amplifier    | KVA                         | 3        |
| Peak amplifier current       | $I_{max}$ (A)               | 10       |
| Number of windings per pole  | $N$                         | 41.38    |
| Biassing current             | $I_b$ (A)                   | 3.35683  |
| Area of copper wire          | $A_{cu}$ (mm <sup>2</sup> ) | 0.791212 |
| Inductance per electromagnet | $L$ (mH)                    | 3.657    |
| RMS current                  | $I_{rms}$ (A)               | 4.74727  |

Table (3) Geometry optimization results for AMB(1), set (1) and (2)

| AMB(1)                |                           |                  |                           |                       |                           |                  |                           |
|-----------------------|---------------------------|------------------|---------------------------|-----------------------|---------------------------|------------------|---------------------------|
| Set (1)               | Design Value              | Limits Low-High  | Optim. Value              | Set (2)               | Design Value              | Limits Low-High  | Optim. Value              |
| w (DV)                | 1.5106 (cm)               | 1.1 – 1.5 (cm)   | 1.3687 (cm)               | w (DV)                | 1.5106 (cm)               | 1.1 – 1.5 (cm)   | 1.4553 (cm)               |
| -----                 | -----                     | -----            | -----                     | w <sub>j</sub> (DV)   | =w                        | 1.1 – 1.5 (cm)   | 1.2418 (cm)               |
| -----                 | -----                     | -----            | -----                     | w <sub>s</sub> (DV)   | =w                        | 1.1 – 1.5 (cm)   | 1.4085 (cm)               |
| g <sub>o</sub> (DV)   | 0.6 (mm)                  | 0.55 – 0.65 (cm) | 0.5502 (mm)               | g <sub>o</sub> (DV)   | 0.6 (mm)                  | 0.55 – 0.65 (cm) | 0.55698 (mm)              |
| ℓ <sub>ax</sub> (DV)  | 13.021 (cm)               | 11 – 13.5 (cm)   | 12.17 (cm)                | ℓ <sub>ax</sub> (DV)  | 13.021 (cm)               | 11 – 13.5 (cm)   | 11.868 (cm)               |
| F <sub>max</sub> (SV) | 5761.3                    | > 5761           | 5770                      | F <sub>max</sub> (SV) | 5761.3                    | > 5761           | 5869.4                    |
| Ivolu (OBJ)           | 1976.7 (cm <sup>3</sup> ) | NON              | 1639.9 (cm <sup>3</sup> ) | Ivolu (OBJ)           | 1976.7 (cm <sup>3</sup> ) | NON              | 1570.5 (cm <sup>3</sup> ) |

Table (4) Geometry optimization results for AMB(2), set (1) and (2).

| AMB(2)                |                           |                 |                           |                       |                           |                 |                           |
|-----------------------|---------------------------|-----------------|---------------------------|-----------------------|---------------------------|-----------------|---------------------------|
| Set (1)               | Design Value              | Limits Low-High | Optim. Value              | Set (2)               | Design Value              | Limits Low-High | Optim. Value              |
| w (DV)                | 0.67913                   | 0.6 – 1.2 (cm)  | 0.6467 (cm)               | w (DV)                | 0.6791                    | 0.6 – 1.2 (cm)  | 0.85418 (cm)              |
| -----                 | -----                     | -----           | -----                     | w <sub>j</sub> (DV)   | =w                        | 0.5 – 1 (cm)    | 0.73240 (cm)              |
| -----                 | -----                     | -----           | -----                     | w <sub>s</sub> (DV)   | =w                        | 0.5 – 1 (cm)    | 0.77749 (cm)              |
| g <sub>o</sub> (DV)   | 0.4 (mm)                  | 0.4 - 0.5 (mm)  | 0.4005 (mm)               | g <sub>o</sub> (DV)   | 0.4 (mm)                  | 0.4 - 0.5 (mm)  | 0.4003 (mm)               |
| ℓ <sub>ax</sub> (DV)  | 4.85826                   | 3 – 6 (cm)      | 5.0512 (cm)               | ℓ <sub>ax</sub> (DV)  | 4.8582                    | 3 – 6 (cm)      | 3.9188 (cm)               |
| F <sub>max</sub> (SV) | 540                       | > 540           | 540.44                    | F <sub>max</sub> (SV) | 540                       | > 540           | 542.36                    |
| Ivolu (OBJ)           | 154.34 (cm <sup>3</sup> ) | NON             | 151.17 (cm <sup>3</sup> ) | Ivolu (OBJ)           | 154.34 (cm <sup>3</sup> ) | NON             | 150.20 (cm <sup>3</sup> ) |

Table (5) Transient-state analysis results for the journal of AMB (1).

| Time (msec) | $F_x$<br>V.Work<br>(N/m) | $F_y$<br>V.Work<br>(N/m) | Power-<br>loss<br>(W/m) | Energy-<br>stored<br>(J/m) | Journal current<br>(A-t) |
|-------------|--------------------------|--------------------------|-------------------------|----------------------------|--------------------------|
| 2           | $-0.547 \times 10^{-4}$  | $0.113 \times 10^{-4}$   | 3.281                   | 0.00652                    | $0.256 \times 10^{-3}$   |
| 4           | $-0.818 \times 10^{-3}$  | $0.184 \times 10^{-3}$   | 40.90                   | 0.08113                    | $0.132 \times 10^{-2}$   |
| 6           | $-0.384 \times 10^{-2}$  | $0.102 \times 10^{-2}$   | 146.4                   | 0.3334                     | $0.293 \times 10^{-2}$   |
| 8           | $-0.113 \times 10^{-1}$  | $0.349 \times 10^{-2}$   | 331.3                   | 0.9008                     | $0.398 \times 10^{-2}$   |
| 10          | $-0.258 \times 10^{-1}$  | $0.912 \times 10^{-2}$   | 608.2                   | 1.935                      | $0.427 \times 10^{-2}$   |
| 30          | -0.2804                  | 0.3368                   | 1119                    | 19.51                      | $0.636 \times 10^{-2}$   |
| 60          | -2.892                   | 1.815                    | 1329                    | 41.22                      | $0.209 \times 10^{-1}$   |

Table (6) Transient-state analysis results for the journal of AMB (2).

| Time (msec) | $F_x$<br>V.Work<br>(N/m) | $F_y$<br>V.Work<br>(N/m) | Power-<br>loss<br>(W/m) | Energy-<br>stored<br>(J/m) | Journal<br>current<br>(A-t) |
|-------------|--------------------------|--------------------------|-------------------------|----------------------------|-----------------------------|
| 2           | $-0.1214 \times 10^{-2}$ | $0.342 \times 10^{-3}$   | 1.494                   | 0.00295                    | $-0.221 \times 10^{-3}$     |
| 4           | $-0.1841 \times 10^{-1}$ | $0.303 \times 10^{-2}$   | 17.92                   | 0.03527                    | $-0.985 \times 10^{-4}$     |
| 6           | $-0.8396 \times 10^{-1}$ | $0.445 \times 10^{-2}$   | 61.29                   | 0.1393                     | $0.254 \times 10^{-2}$      |
| 8           | -0.2330                  | $-0.13 \times 10^{-1}$   | 132.5                   | 0.3627                     | $0.842 \times 10^{-2}$      |
| 10          | -0.4924                  | $-0.86 \times 10^{-1}$   | 232.5                   | 0.7516                     | $0.16 \times 10^{-1}$       |
| 30          | 1.504                    | -8.338                   | 287.9                   | 5.189                      | $0.234 \times 10^{-1}$      |
| 60          | 25.40                    | -34.04                   | 140.3                   | 7.213                      | $-0.441 \times 10^{-2}$     |

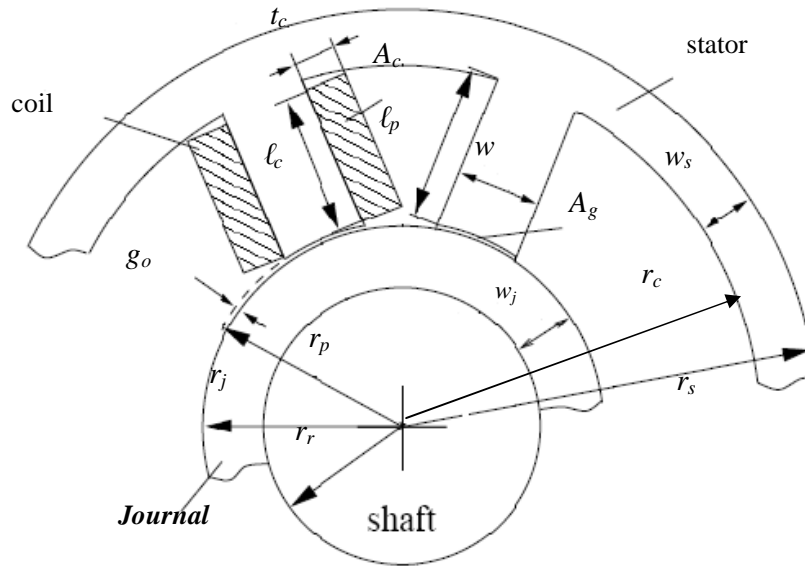


Figure (1) AMB geometry parameters.

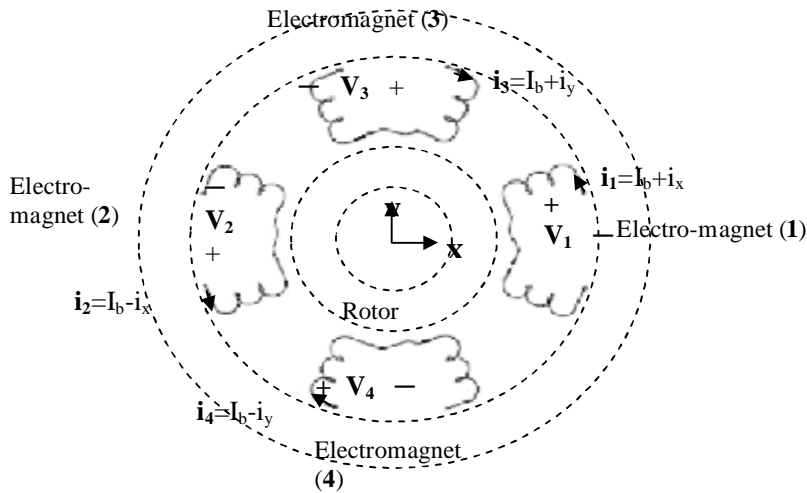


Figure (2) Circuit diagram of a 4-electromagnet radial AMB.

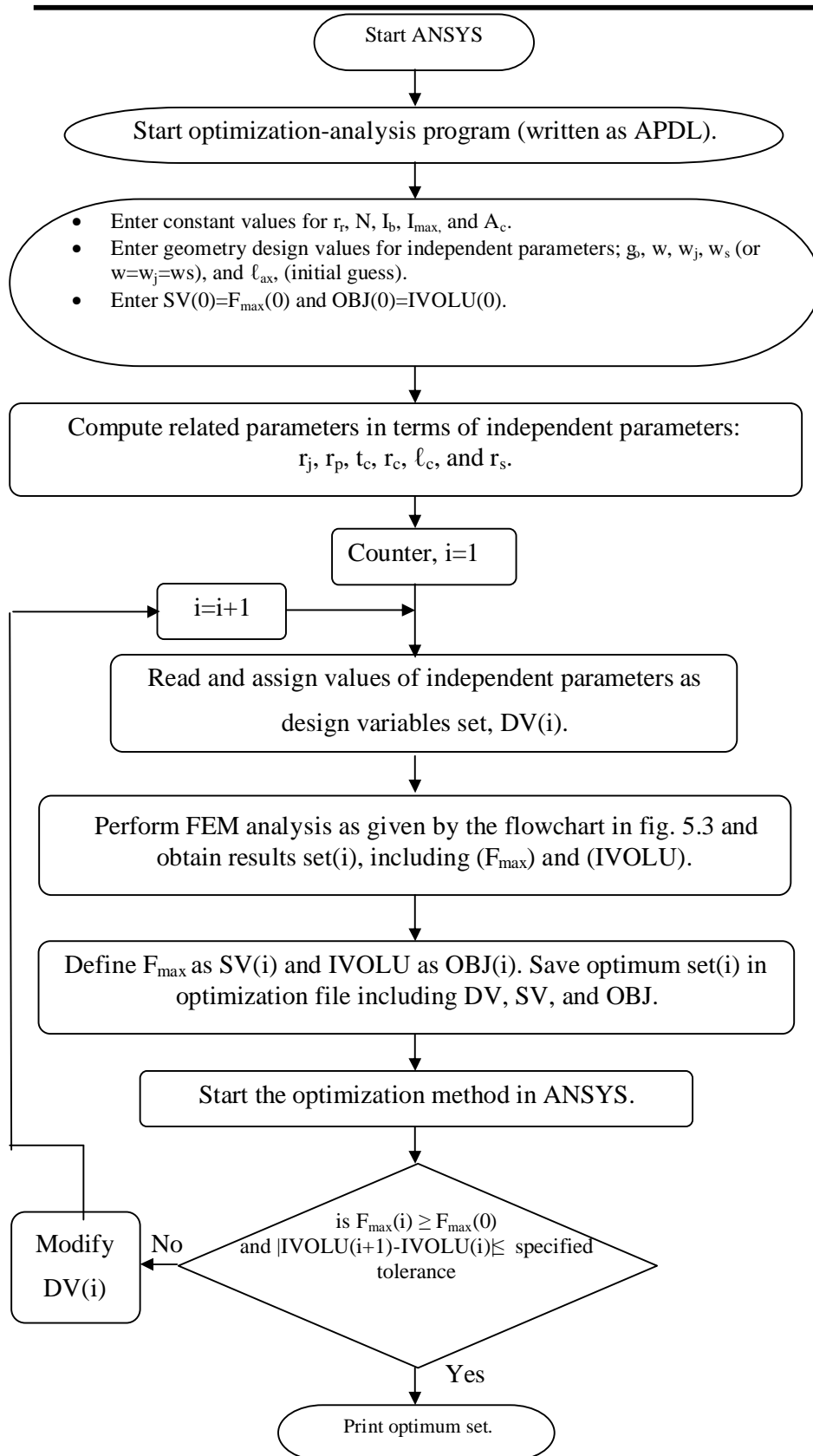


Figure (3) Flowchart representing the geometry optimization program.

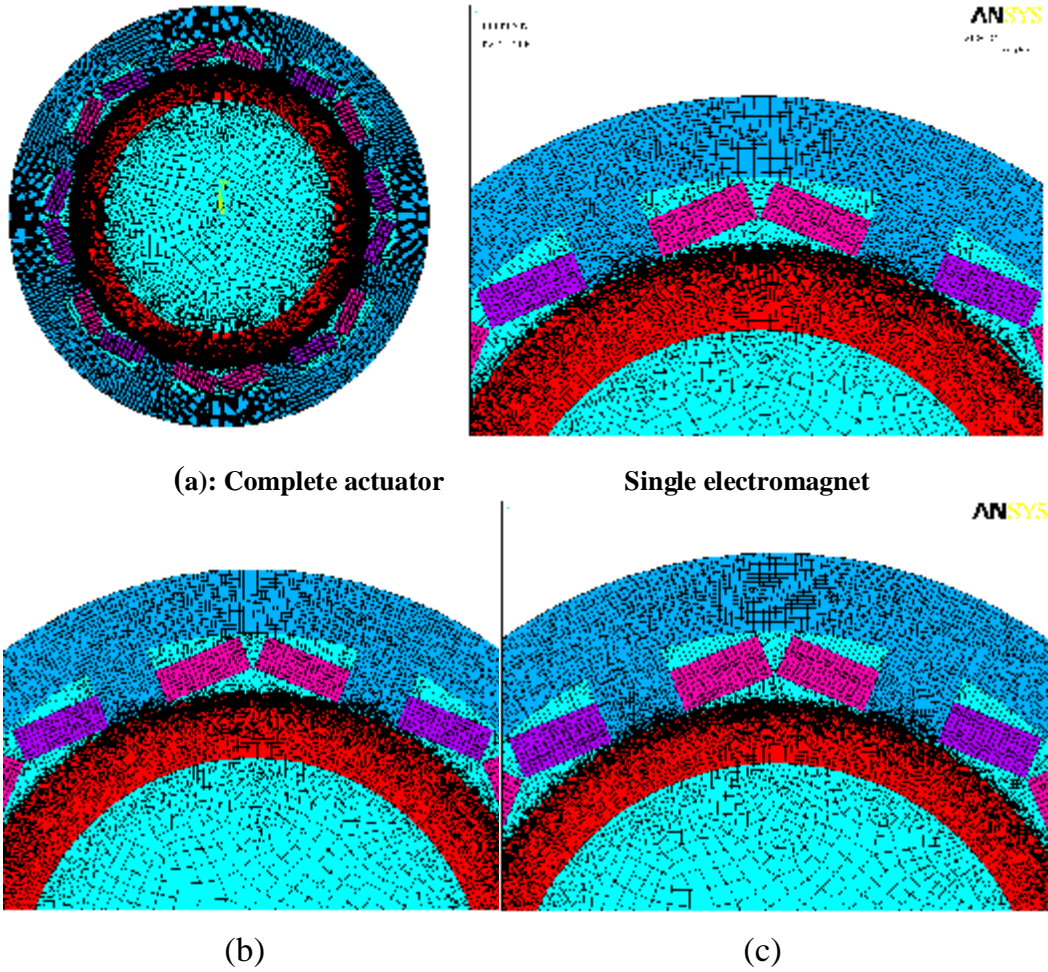


Figure (4) AMB(1), (a) designed geometry, (b) and (c) optimized geometry set (1) and (2) respectively.

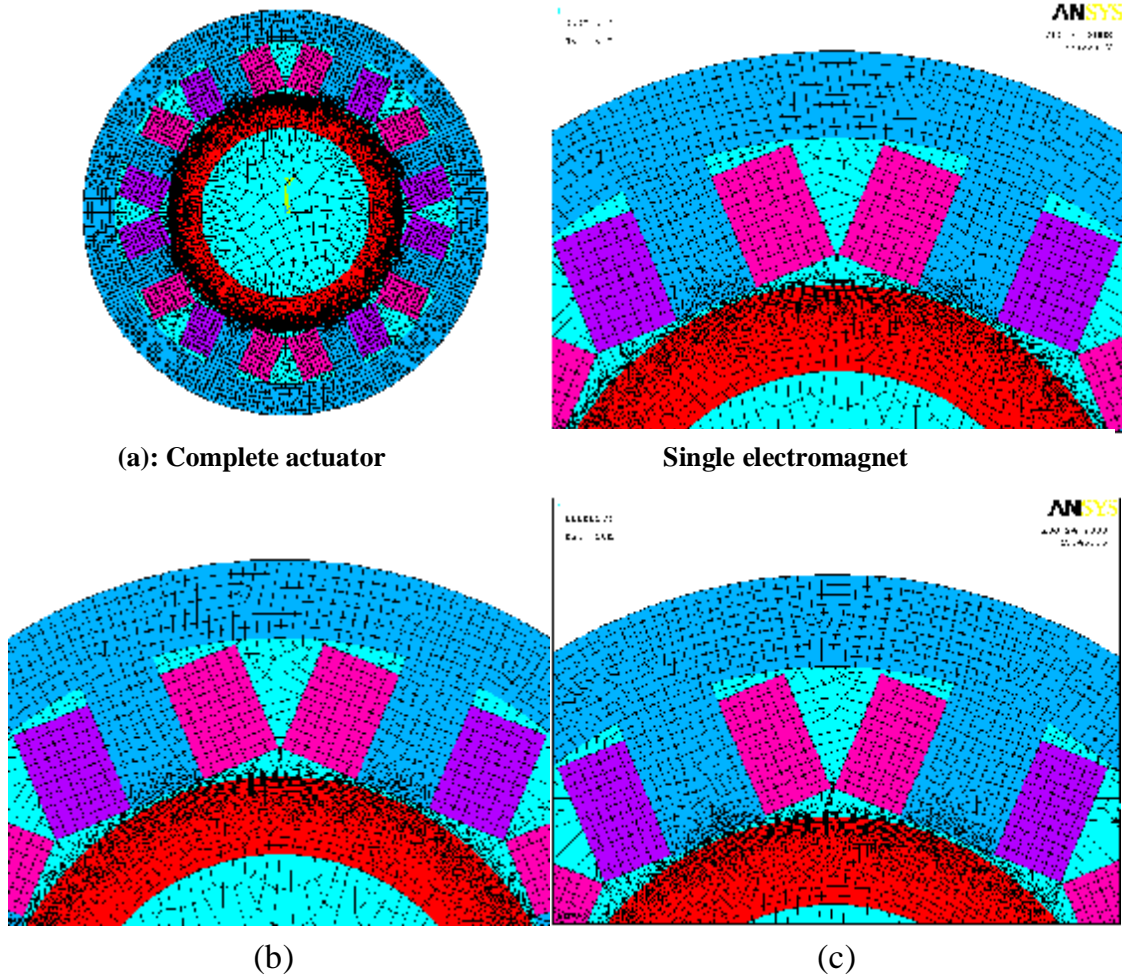
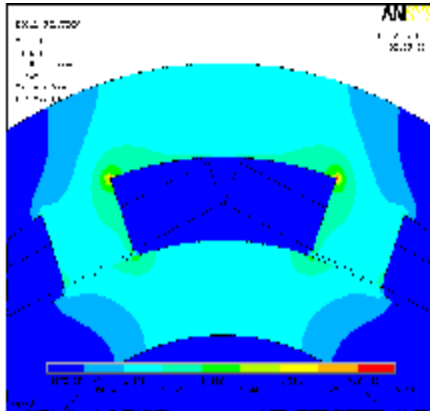
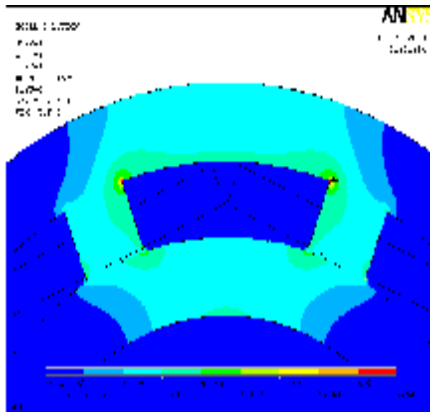


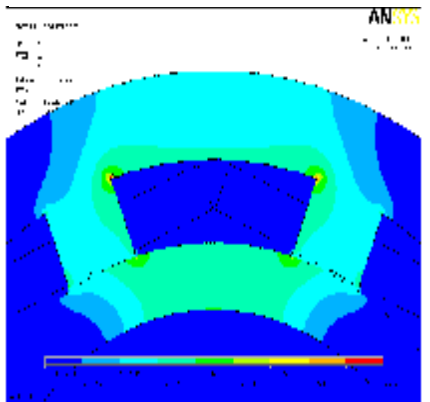
Figure (5) AMB(2), (a) designed geometry, (b) and (c) optimized geometry set (1) and (2) respectively.



(a): Single electromagnet

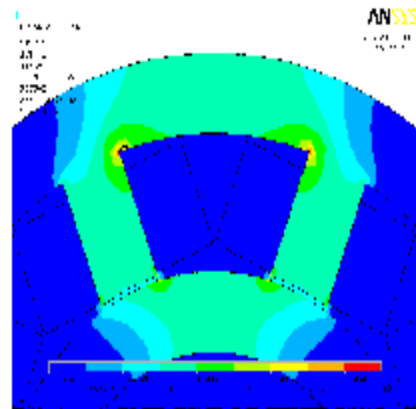


(b): Single electromagnet

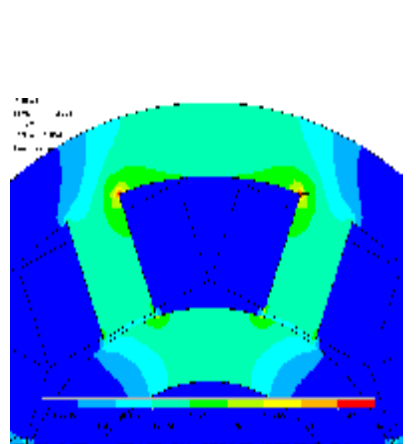


(c): Single electromagnet

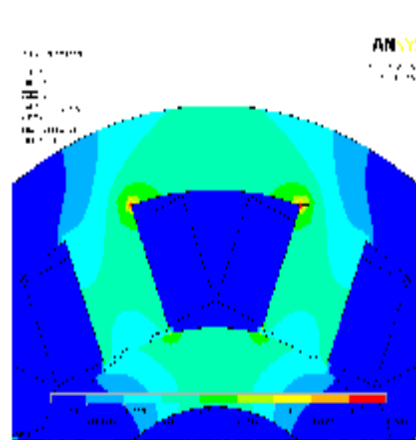
Figure 6: Flux density distribution for AMB (1), (a) designed geometry (b) and (c) optimized geometry, set (1) and (2) respectively.



(a): Single electromagnet



(b): Single electromagnet



(c): Single electromagnet

Figure 7: Flux density distribution for AMB (2), (a) designed geometry (b) and (c) optimized geometry, set (1) and (2) respectively.

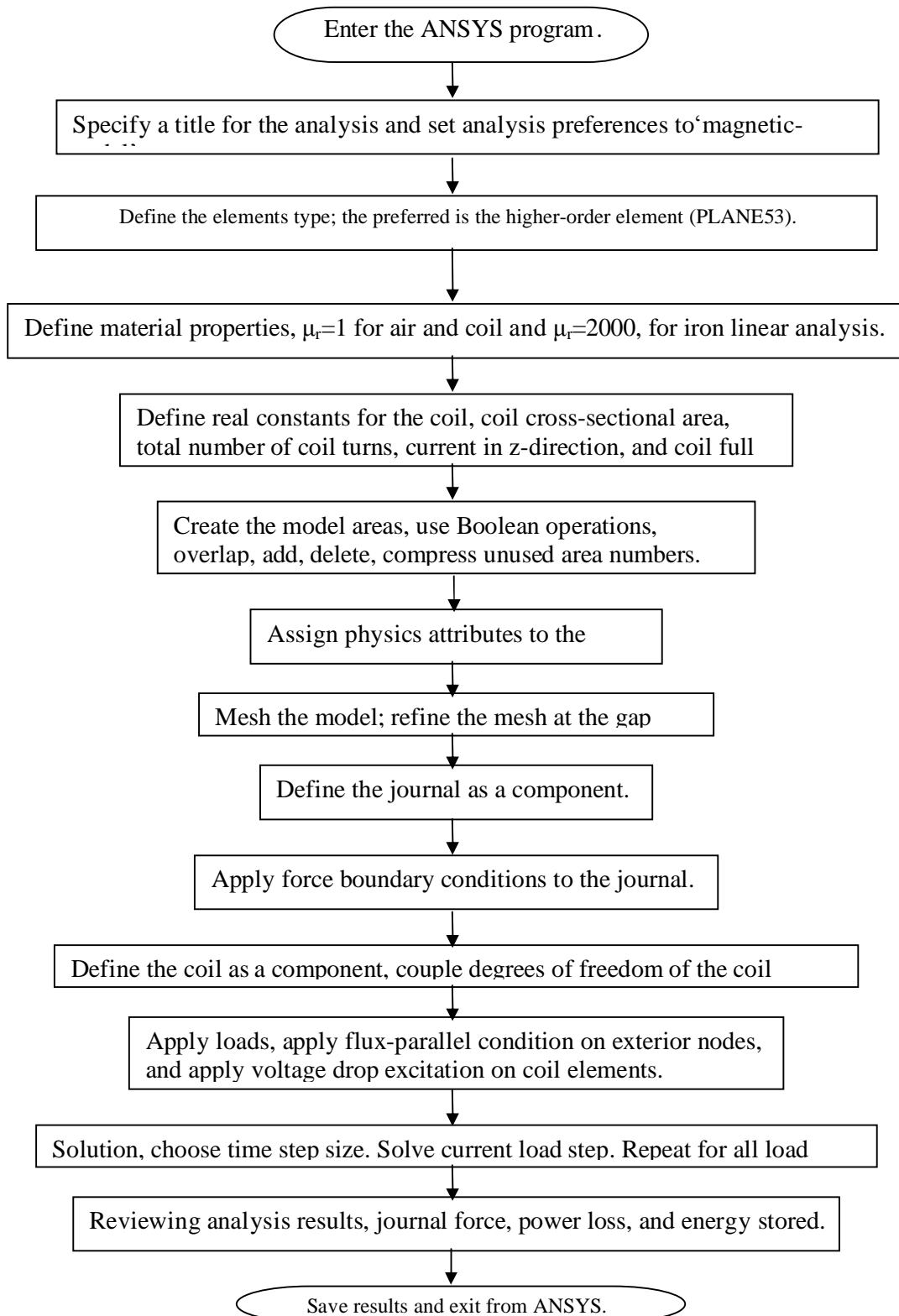


Figure (8) Transient-state analysis program of AMB.

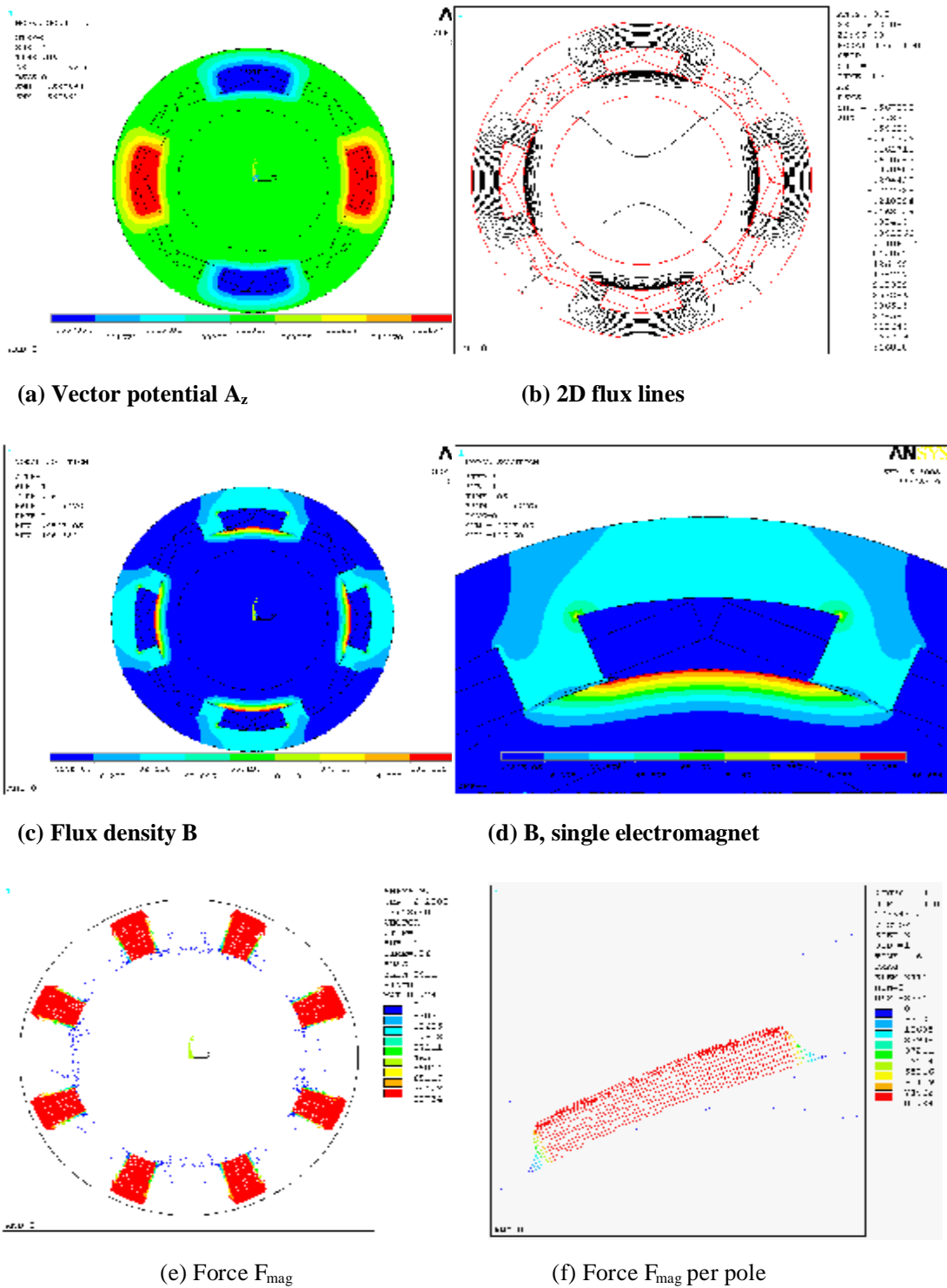
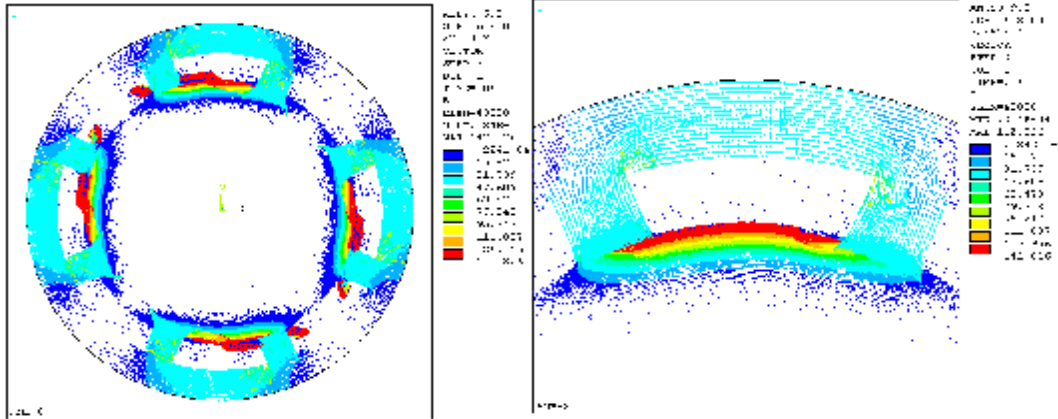


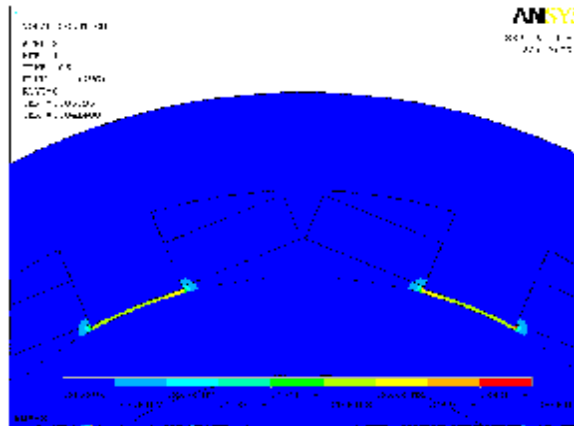
Figure (9) Transient-state analysis of AMB(1).



(a) Flux density  $B$ , vector plot.

(b)  $B$ , single electromagnet.

(c) Magnetic flux intensity  $H$ , single electromagnet.



(d) Current density  $J_z$ .

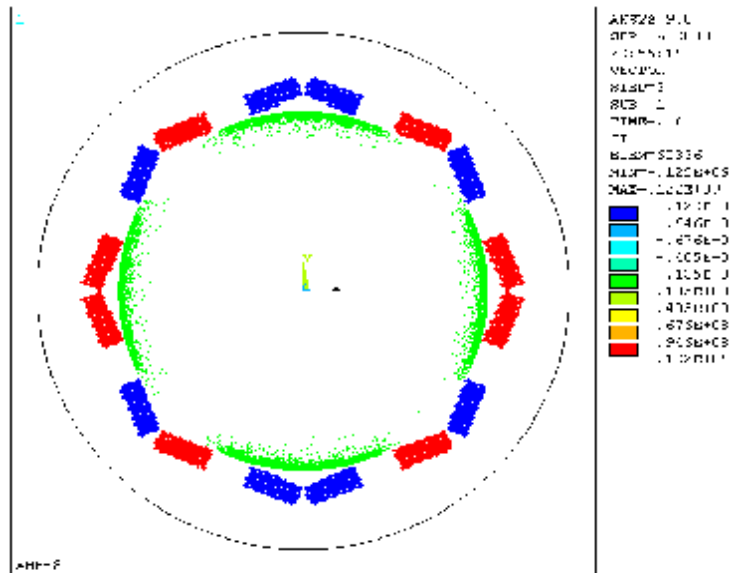
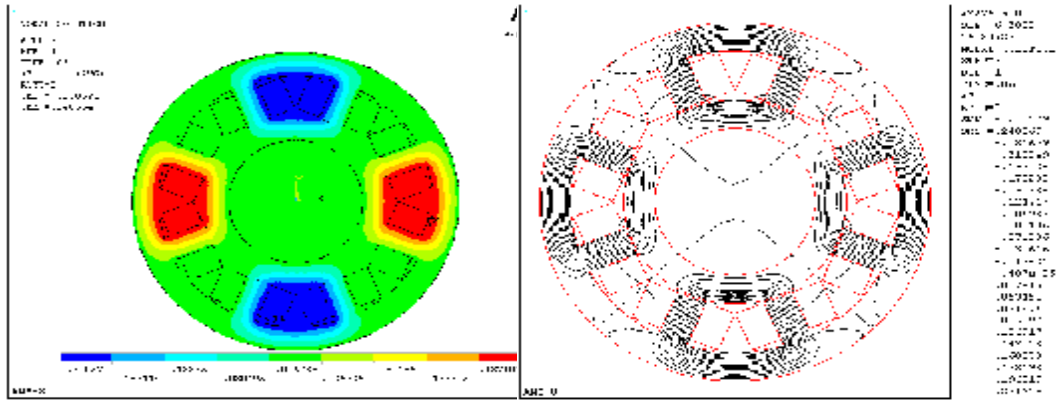
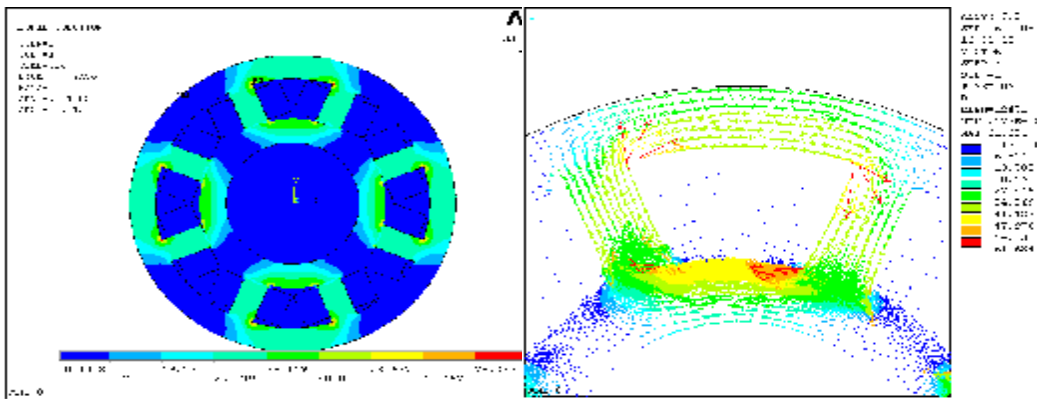


Figure (10) Transient-state analysis of AMB (1).

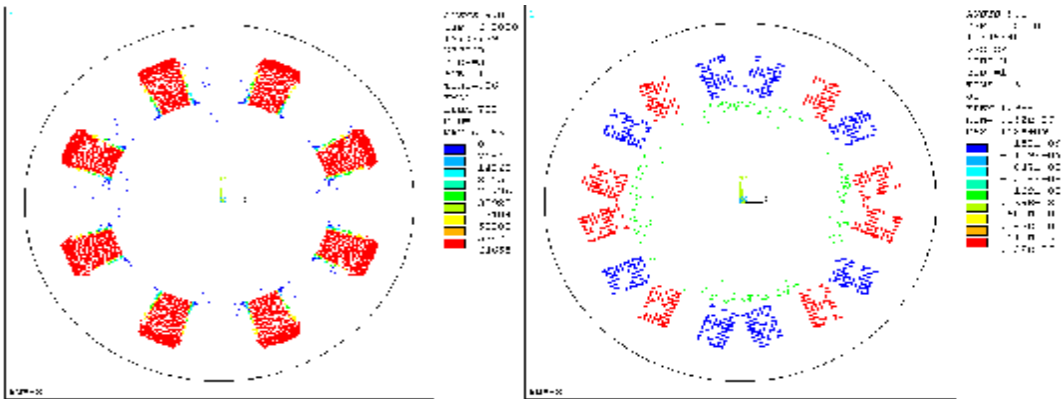


(a) Vector potential  $A_z$

(b) 2D flux lines



(c) Flux density  $B$ , contour plot. (d)  $B$ , vector plot for  
single electromagnet.



(e) Force  $F_{mag}$

(f) Current density  $J_z$

Figure (11) Transient-state analysis of AMB (2).